

The Atomic Force Spectroscopy as a Tool to Investigate Surface Forces: Basic Principles and Applications

F. L. Leite^{1,2}, L. H. C. Mattoso¹, O. N. Oliveira Jr², P. S. P. Herrmann Jr^{*,1}

¹National Nanotechnology Laboratory for Agriculture, Embrapa Agricultural Instrumentation (LNNA), P. O. Box 741, São Carlos, 13560-970, SP, Brazil.

²Institute of Physics of São Carlos, University of São Paulo (USP), P. O. Box 369, São Carlos, 13560-970, SP, Brazil.

Atomic force microscopy (AFM) has been useful to investigate materials performance, processes, physical and surface properties at the nanometer scale. In addition to the standard AFM, which measures surface topography, many accessories have been developed to obtain specific additional information. In this chapter, we shall concentrate on atomic force spectroscopy (AFS), which derived from AFM and is used to measure surface forces through force curves. The latter curves have become an important tool to study materials properties, such as elasticity, surface charge densities and wettability. With AFS one probes interactions at the nanometer scale, especially van der Waals interactions and double-layer forces. A brief theoretical background is included, and we comment on the large variety of measurements involving AFS.

Keywords: atomic force spectroscopy; atomic force microscopy, interactions forces; surface forces.

1. Introduction

The learning of atomic and molecular scale concepts in chemistry and physics may be impaired by the difficulty of many students in visualizing atoms and molecules [1,2]. Such abstract concepts may now be studied with hands-on experience [3] if students become familiar with state-of-the-art microscopy techniques. Of special relevance are the scanning tunneling microscope (STM) [4], the atomic force microscope (AFM) [5], and the family now referred to as the scanning probe microscopes (SPM), which are based on various types of interactions, *e.g.* ionic repulsion, electrostatic, van der Waals, magnetic, frictional interactions [6]. This family of SPM microscopes shares certain features: there is a probe and a surface that are brought into close proximity and then scanned relative to each other by means of piezoelectric devices. Suitable detection circuitry is required to monitor the interaction between the tip and the surface. The nature of the interaction to be investigated defines the type of SPM.

AFM studies can be divided into topographical applications (imaging modes) [7,8] and force curves or so-called atomic force spectroscopy (AFS), in which forces are measured as a function of distance [9,10]. The first group consists in getting an image of the sample surface to observe its structural or dynamic features. It has been applied to a variety of surfaces including semiconductors [11], biological systems [6,12,13], nanostructures [14] and polymers [15,16], with resolution reaching the nanometer range and in some instances the atomic scale. The second approach, AFS [17], allows one to study inter and intramolecular forces, and manipulate samples following dissection, dragging and cut. AFS has been used to study biological systems [18,19], polymers [20,21] and interfacial phenomena in various systems [9,22-24].

The aim of this review is to provide a glimpse of the potential and limitations of AFS, especially for applications in materials science to study surface forces.

* Corresponding author: e-mail: herrmann@cnpdia.embrapa.br, phone: +55 1633742477.

2. Atomic Force Microscopy (AFM)

This section briefly introduces the basic elements of an AFM and its principle of operation. In AFM, one scans the sample surface with a sharp probe or tip, situated at the apex of a flexible cantilever that is often a diving board or V-shaped, usually made of silicon. The AFM utilizes a piezoelectric scanner that moves the sample in 3 dimensions by a subnanometer amount when a voltage is applied (Fig. 1a). To form an image, the tip is brought close to the sample and raster-scanned over the surface, causing the cantilever to be deflected due to probe-sample interactions. A line-by-line image of the sample is formed as a result of this deflection, which is itself detected using laser light reflected off the back surface of the cantilever onto a position-sensitive photodiode detector [25,26]. Forces acting between the sharp probe (tip) placed in close contact with the sample result in a measurable deformation of the cantilever to which the probe is attached. The cantilever bends vertically upwards or downwards because of repulsive or attractive interactions, respectively. The forces acting on the tip vary, depending on the sample nature, imaging mode and conditions used in the measurements.

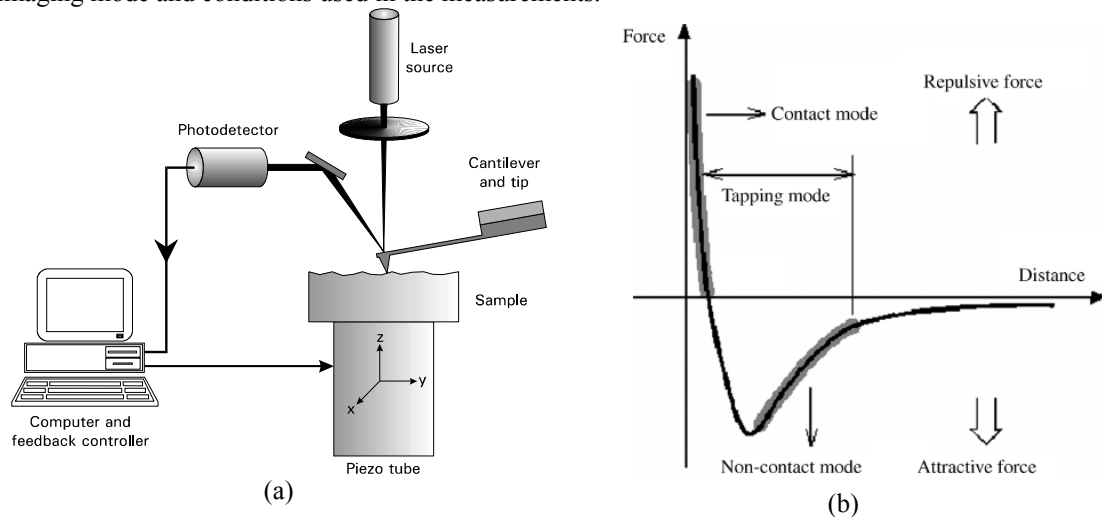


Figure 1. (a) Schematic representation of the main components of an atomic force microscope (AFM) and (b) illustrative force vs distance curve between the scanning tip and sample that reflects the main interaction during AFM measurements. The ranges of AFM regimes are indicated.

In AFM, a number of imaging modes are available [27,28]:

- i. *Constant force imaging*: during the scanning process, the force between the probe and the surface is kept constant by maintaining a constant cantilever deflection with a feedback loop controlled by the computer. The displacements of the probe relative to the surface required to keep the force constant are amplified to generate an image. This is the most common mode of operation;
- ii. *Constant height mode*: the probe is positioned close to the surface. During scanning, the deflections of the cantilever are measured and amplified in order to produce an image. Because the feedback loop is disconnected this mode of operation permits higher scan rates;
- iii. *Constant force gradient mode*: this mode of operation can be used to detect small attractive forces. The cantilever is excited at its resonant frequency and interactions between tip and the sample alter the resonant frequency. Such effects are measured and used to generate images of the sample;
- iv. *Intermittent contact mode (Tapping mode)*: In the tapping mode, the cantilever is excited by an electrical oscillator to amplitudes of up to ca. 100 nm, so that it effectively bounces up and down (or taps) as it travels over the sample. The oscillation amplitude is measured as a root mean

square (RMS) value of the deflection detector signal. The feedback system is set to detect the perturbation on the oscillation amplitude caused by intermittent contact with the surface.

A three-dimensional image of a surface is obtained with AFM under the assumption that the interaction between tip and sample as function of separation is the same at all points on the surface; thus any given force corresponds to a particular separation. Fig. 1b represents the tip-sample interaction force ($F(D)$) with the ranges of AFM operation modes. At short distances, the cantilever mainly senses interatomic forces: the very short range (≈ 0.1 nm), repulsive forces, and the longer-range (up to 10 nm), van der Waals forces. At very small tip-sample distances, a strong repulsive force appears between the atoms of the tip and those of the sample. This repulsive force occurs between any two atoms or molecules that approach so closely that their electron orbitals begin to overlap. It is thus a result of the Pauli Exclusion Principle [29]. When this repulsive force is predominant in an AFM set-up, tip and sample are considered to be in "contact" (regime of contact mode).

The total intermolecular pair potential is obtained by assuming an attractive potential, (C_1/D^6) , and a repulsive potential, (C_2/D^{12}) . Superimposing the two gives an expression for the well-known Lennard-Jones potential: $U = C_2/D^{12} - C_1/D^6$, where C_1 and C_2 are the corresponding coefficients for the attractive and repulsive interactions.

This force sensing ability means that AFM can be also used for measuring surface forces, as will be described in Section 3.

3. Atomic Force Spectroscopy (AFS)

Atomic force microscopy can be used to determine - at every location of the sample - the dependence of the interaction on the probe-sample distance [30]. To determine the spatial variation of the tip-sample interaction, force curves may be recorded at a large number of locations with atomic force spectroscopy (AFS). Using AFS it is possible to obtain the following pieces of information: (i) magnitude of the force which depends on long-range attractive and adhesive forces, (ii) point of tip-sample contact, (iii) tip-sample contact area, and (iv) elastic modulus and viscoelasticity of thin and thick films. For more details see reference [27,31,32].

3.1 Local Force Spectroscopy (LFS)

With commercially available cantilevers, AFM may be used to measure forces accurately down to ~ 10 pN [33]. Hence, it is possible to investigate complex inter- and intra-molecular interactions, and the ranges, magnitudes and time-dependence of rupture forces, as well as the mechanical properties of molecules and the strength of individual bonds [34,35]. There are several features of AFM that make it ideal for force sensing, including: sensitivity of the displacement of ca. 0.01 nm; small tip-sample contact area of about 10 nm^2 , and the ability to operate under physiological conditions [36]. In order to analyze force-mapping experiments, one has to understand how single-point force-distance curves are obtained and the information provided regarding tip-sample interaction.

In local force spectroscopy (LFS), the force curve is determined at a particular location on the sample surface. This method is shown schematically in Fig. 2. At the first stage of cycle (A), a large distance separates the tip and the sample, there is no interaction between them and the cantilever remains in a noninteracting equilibrium state. As separation decreases, the tip is brought into contact with the sample at a constant speed until it reaches a point close to the sample surface. As the sample moves towards the tip various attractive forces pull on the tip (long and short range forces). Once the total force acting on the tip exceeds the stiffness of the cantilever it jumps into contact with the sample surface (jump-to-contact) (B-C). At point (D), the tip and sample are in contact and deflections are dominated by mutual electronic repulsions between overlapping molecular orbitals of the tip and sample atoms (A - D is the approach curve). In this region, which is typically linear, the elastic properties of the sample can be measured. The subsequent sample deformation is consistent with elastic asperity deformation and/or the

presence of a thin contamination layer. The slope of the curve in the contact region is a function of the elastic modulus and geometries of the tip and sample, and will only approach unity for rigid systems [37-39].

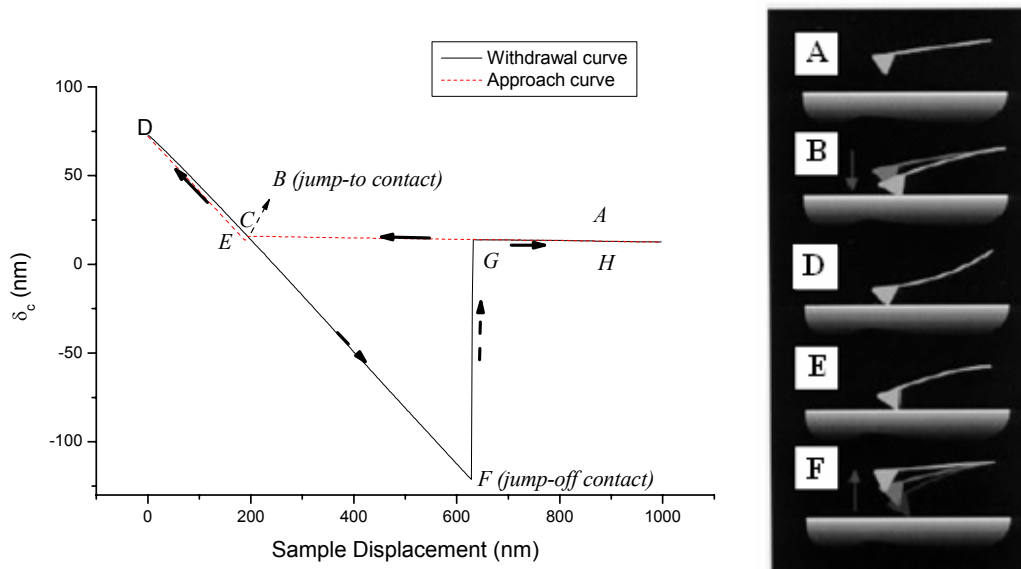


Figure 2. (a) Force-displacement curve on a conducting polymer (poly-*o*-ethoxyaniline) illustrating the points where jump-to-contact (approach) and jump-off-contact (withdrawal) occur and the maximum values of the attractive forces (pull-on force and pull-off force) (adapted from the [40]).

Given a calibrated sensor response, the shape of segment (C-D) indicates whether the sample is deforming in response to the force from the cantilever. This slope can be used to infer the sample hardness or indicate a differing sample response at different loading charges, which result from a transition from elastic to plastic deformation. The segment (D-E) represents the reverse of segment (C-D). If both segments are straight and parallel to each other, there is no additional information content. If they are not parallel, the hysteresis gives information about the plastic deformation of the sample [41].

During withdrawal, adhesion or bonds formed during contact with the surface cause the tip to adhere to the sample up to some distance beyond the initial contact point on the approach curve (E-F). As the piezotube continues retracting, the spring force of the bent cantilever overcomes the adhesion forces, and the cantilever pulls off sharply, springing upwards to its non-deflected or noncontact position (G). Finally, the tip completely loses contact with the surface and returns to its starting equilibrium position (H) (D-H is the withdrawal curve).

Approach and withdrawal curves can be divided roughly into three regions: the contact line, the non-contact region and the zero line. The zero line is obtained when the tip is far from the sample and the cantilever deflection is close to zero (when working in liquids, this line gives information on the viscosity of the liquid [32]). When the sample is pressed against the tip, this line may provide information on sample stiffness. The most interesting regions of the force curve are the two non-contact regions, containing the jump-to-contact and the jump-off-contact. The non-contact region in the approach curve gives information about attractive (van der Waals or Coulomb force) or repulsive forces (van der Waals in some liquids, double-layer, hydration, and steric force) before contact. This discontinuity (jump-to contact) occurs when the gradient of the tip-sample force exceeds the elastic constant of the cantilever (pull-on force). The non-contact region in the withdrawal curve contains the jump-off-contact, a discontinuity that occurs upon withdrawing the sample and the cantilever elastic constant is greater than the gradient of the tip-sample adhesive forces (pull-off force).

A convenient way to measure forces accurately is to convert them into deflections of a spring, according to Hooke's law:

$$F = -k_c \Delta z \quad (1)$$

where the deflection Δz is determined by the acting force F and the spring constant of the cantilever, k_c . Although cantilevers have spring constants defined by the manufacturer, the actual spring constant may deviate from this value by an order of magnitude. It is therefore necessary to determine the spring constant experimentally. This may involve determining the resonant frequency of the cantilever before and after adding a small mass to the tip [42] and measuring ascertaining the unloaded resonant frequency considering the cantilever's density and dimensions [43], or thermal fluctuation of the cantilever [44,45].

In Eq. (1) the acting force leads to a total bending Δz of the cantilever and surface. The real probe-sample distance is then given by:

$$d = z - \Delta z \quad (2)$$

where z is the distance between the sample surface and rest position of the cantilever and Δz is the sum of the cantilever deflection, δ_c , and sample deformation, δ_s [32]. Since one does not know, in advance, the cantilever deflection and the sample deformation, the distance that can be controlled is the displacement of the piezotube. Therefore, the raw curve obtained with an AFM should be named "force-displacement curve" rather than "force-distance curve" [32]. This latter term should be employed only for curves in which the force is plotted vs the true tip-sample distance. Fig. 3a shows a force-distance curve obtained in aqueous solution to detect hydration forces on thin films of conducting polymers, e.g. polyanilines (PANI). The force-distance curve or deflection-distance curve of Fig. 3a features a repulsive force at a distance ≈ 9 nm of the sample, which is attributed to hydration forces. This type of interaction was also detected by force-displacement curves on PANI derivatives, i.e., poly(*o*-ethoxyaniline) (POEA) films [46]. Once the optimum conditions were established, the interactions were monitored *in situ* using the setup illustrated in Fig. 3b, with force curve measurements being obtained immediately after the injection of contaminants.

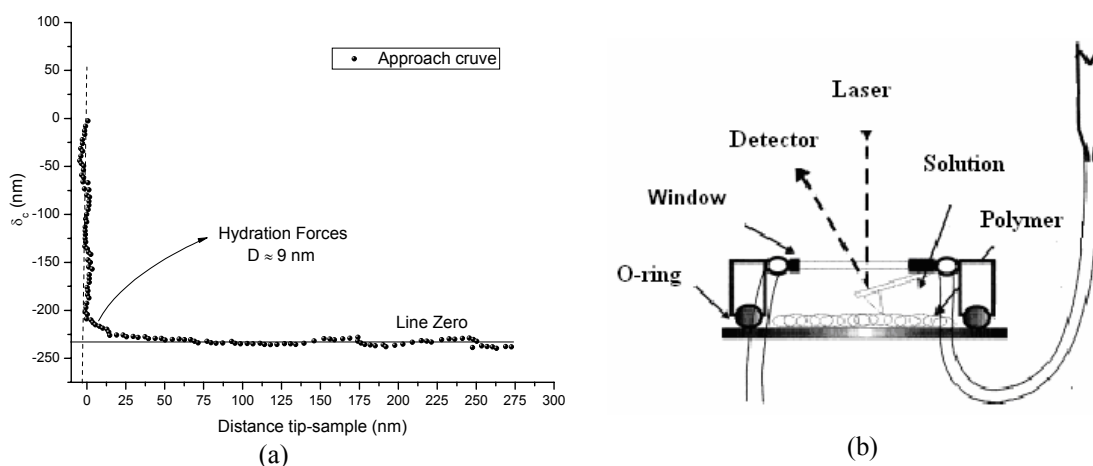


Figure 3. Typical force-distance curve (approach curve) for POEA film in aqueous solution with concentration of CuSO_4 of 2.5 mol L^{-1} ; (b) Schematic diagram of the experimental setup used for *in situ* AFS. Using this setup, the liquid can be injected into or removed from the liquid cell without perturbing the system.

The evolution of curve forces with time is also important for the analysis of environmental sensors [47]. AFS experiments in solution showed that water ages upon exposure to air. Fig. 4a is a typical force curve obtained for a mica surface ($\text{pH} \approx 7.0$) in a cell filled with pure water, which result in van der

Waals interactions for short times ($<1\text{h}$). The presence of impurities in the cell affected the force curves. For longer times, repulsive double-layer forces dominate (Fig. 4b) until the force curve is practically purely repulsive (t''). Ageing of the water is accompanied by a decrease in pH, which then increases the charge of the silicon nitride tip (whose isoelectric point is pH 6.3), whereas mica is negatively charged. The net result is an increase in the repulsive, double-layer force.

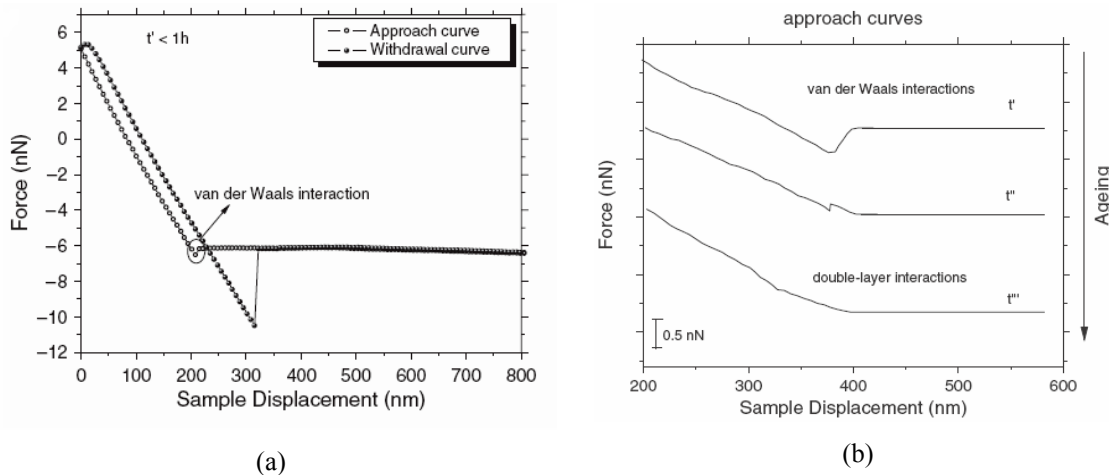


Figure 4. Typical force curve for an AFM tip and mica sample immersed in water and (b) schema (approach curves) showing water ageing for various periods of time (increasing in the direction $t < t' < t''$). The difference between each of two times, $t - t'$ or $t' - t''$ is 2h. ([47] Reprinted from Sensor Letters, Borato *et al.*, 2006, with permission from the American Scientific Publishers (ASP). All rights reserved).

3.2 Force Imaging Spectroscopy (FIS)

In the mid 1990s, the idea of collecting data from force-distance curves obtained from many points on a sample was introduced to produce a map of the tip-surface interactions [48,49]. Layered imaging is an SPM technique in which several measurements of cantilever deflection are made at each image pixel. Each measurement is preceded by a deflection being read and the result stored. When all measurements for the current pixel are completed, the process is repeated at the next pixel and so on through the scanned area. The resulting spatial maps represent the lateral variation of adhesion force due to material inhomogeneities and the surface topography [50]. The resulting three-dimensional data set may be displayed as in Fig. 5a. Each horizontal layer is an image representing the measurements taken throughout the scanned area at a specified height z . Since several measurements are conducted at each pixel, the data set can be also processed vertically to yield the force distance curve at each pixel. This Force Imaging Spectroscopy (FIS) mode of AFM can thus be used to measure adhesion [51], hardness or deformability of samples and surface charge heterogeneities [52]. Interestingly, many probe/sample interaction mechanisms can be studied.

Fig. 5a shows an image of a submonolayer of intercellular adhesion molecule-1 (ICAM-1) in the adhesion mode [53]. The authors showed that when the force set point was raised, a substantial increase (25%) occurred in the number of bright pixels, indicating that the probability of reaching adhesive contact was increased. During imaging of this surface in the adhesion mode, the force set point on maximum force was changed. The image consists of 100 lines, and on line #50 the force set point was increased from 60 to 80 pN, while on line #75 it was decreased to 40 pN. Adhesion maps can also be obtained with AFS by measuring the vertical displacement of the sample—driven by the piezoscanner—and the deflection of the cantilever, with respect to its position at rest on several points of the surface [54]. Force curves are digitally acquired at 100 points or more, equally spaced from each other over the scanned area of the surface. For the map in Fig. 5b, each force curve comprised a row of a maximum of 250 data

points acquired during the vertical movements of approach and retraction of the cantilever, and software was used to create the adhesion maps.

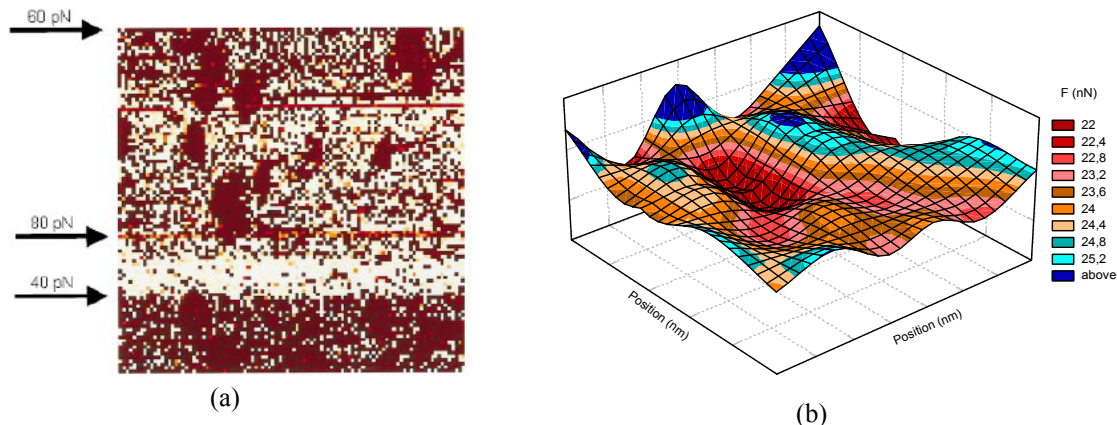


Figure 5. (a) Adhesion image (force range: 0–300 pN) ([53] Reprinted from Biophysical Journal, Willemsen *et al.*, 1999, with permission from the Biophysical Society). (b) Adhesion map illustrating the variability of adhesion forces onto a polyaniline surface in contact with a pesticide (atrazine).

Furthermore, AFS allowed one to distinguish between nonspecific adhesion and specific interactions (pesticide) as shown in Fig. 5b. This adhesion map was acquired with a thin film of POEA in contact with atrazine for 2 hours. The interaction is not homogenous, as indicated by the adhesion map, and the regions with higher forces are those that were probably most contaminated by atrazine, since the tip was functionalized (self-assembled) with the protein bovine serum albumin (BSA) where the interaction is higher and specific. This technique is known as Chemical Force Microscopy (CFM), which is further detailed in Section 3.3. Interactions between pesticides and conducting polymers were also analyzed through morphological changes [55].

AFS may be used to study nanoscale surface chemistry and morphology changes caused by different chemical treatments. The adhesion maps in Fig. 6 show the distribution of adhesion force (F) magnitude on sisal fibers [56]. Each adhesion map represents a scan range of $3\ \mu\text{m}$ and the adhesion distribution on the surface is associated with the chemical heterogeneity of the surface. The force curve measurements provided further information on the changes caused by benzylation of the sisal fibers. For more details, see ref. [56].

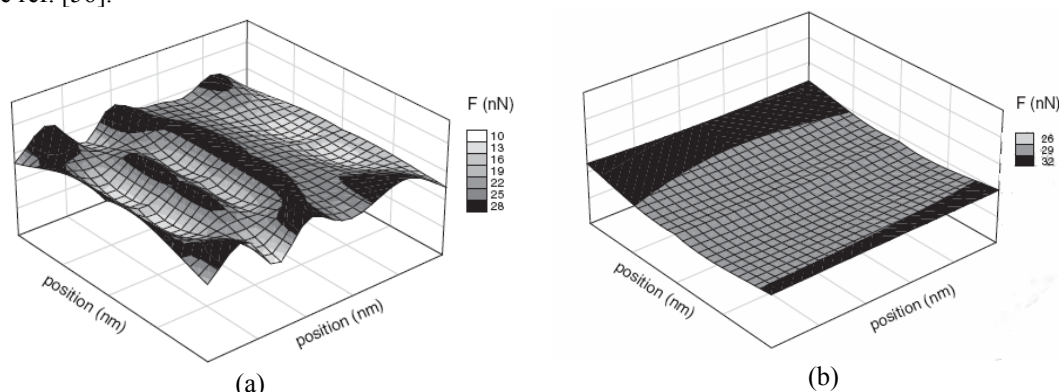


Figure 6. Adhesion force (F) maps (scan size: $3\ \mu\text{m}$) of (a) sisal surfaces treated with 40% NaOH and (b) benzylated sisal for 0.5 hour ([56] Reprinted from J. Nanosci. Nanotechnol., Leite *et al.*, 2006, with permission from the American Scientific Publishers (ASP). All rights reserved).

3.3. Chemical Force Microscopy (CFM)

Adhesion is governed by short-range intermolecular forces, which can be controlled in many cases by appropriate surface modification. This provides a specific chemical function on the probe surface, thus leading to Chemical Force Microscopy (CFM) [57-61]. CFM has been used to evaluate the strengths of specific forces of attraction directly and add chemical discrimination to a mechanical surface probe [62]. One possible way to functionalize the AFM tip is to cover it with an ordered monolayer of organic molecules (a self-assembled monolayer) (Fig. 7a). The force of interaction can be estimated from the excess force required to pull the tip free from the surface. Incidentally, the functionalization of the cantilever surface is another methodology to be exploited in biosensors [63]. The development of CFM has enabled the investigation of adhesion [64,65] and friction [66,67] between surfaces in close, molecular contact and the measurement of nanometer-scale tribological phenomena [68]. Fig. 7b shows the schematic diagram of a functionalized surface with an enzyme (shikimate kinase) [69], used to evaluate the competitive binding interactions between an enzyme immobilized on the tip and two ligands, one immobilized on a surface and the second in free solution. The authors showed that adhesion forces arise predominantly from specific interactions between the immobilized enzyme and surface-bound adenine derivative. The binding of three pairs of specific antigen/antibody systems was studied, namely: BSA, tobacco etch virus capsid protein, and tobacco mosaic virus capsid protein and their respective antibodies [70]. The authors managed to monitor the antigen/antibody binding process *in situ* in real time.

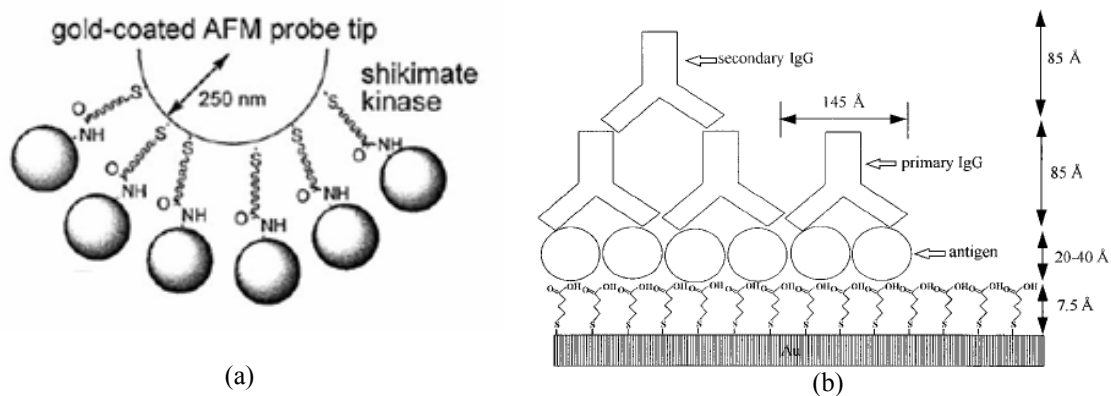


Figure 7. (a) Schematic diagram of the CFM experiment, showing an enzyme bound to the AFM tip ([69] Reprinted from Biophysical Journal, Fiorini *et al.*, 2001, with permission from the Biophysical Society) (b) Schematic diagram of protein immobilization and antigen/antibody complex formation ([70] Reprinted from Langmuir, Browning-Kelley *et al.*, 13, 343, ©1997 with permission from Elsevier).

3.4. AFM Colloidal Probe Technique

The identification of the factors controlling adhesion and the possible development of adhesion-free surfaces can potentially benefit from direct measurements of the strength of adhesive interactions. A number of studies have been carried out using the surface force apparatus technique (SFA) [71]. However, SFA requires molecularly smooth cylindrical samples with a radius of the order of 1 cm. Thus, AFM has provided an alternative for measuring surface forces, which does not require a large smooth cross section. Of special interest is the use of colloid probes, formed by attaching a single particle in the size range 1–20 μm to the cantilever [72-74]. This technique, known as the “colloid probe technique”, was first devised by Ducker [75]. A recent development is the application of the colloidal probe technique to study interactions between a colloidal particle and a bubble [76]. The technique allows the measurement of forces between surfaces of known geometry in a way that facilitates the theoretical analysis of the results. An example of a cantilever with an attached particle is shown in Figure 8, with a silica microsphere glued to the end of an AFM tip. The glue must be insoluble in the solvent in which

interactions are going to be studied, and it should be rigid so that the deformation during the measurement is minimized [77].

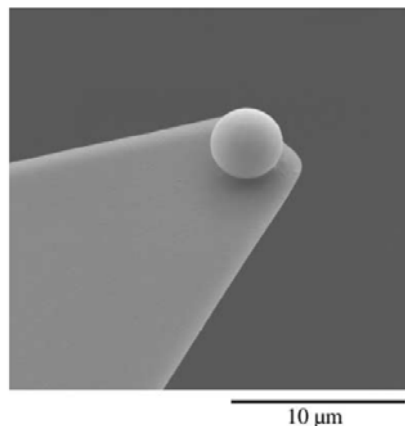


Figure 8. (a) Scanning electron micrograph of silanized silica microsphere glued to the end of a tipless AFM cantilever ([77] Reprinted from Particle & Particle Systems Characterization, Kappl *et al.*, 2002, with permission from the Wiley-VCH Publishers, Inc.)

Bowen *et al.* [73] used AFM to quantify the adhesive interaction between a silica sphere and a planar silica surface and found that the adhesion of such surfaces is a complex phenomenon, with non-DLVO (Derjaguin-Landau-Verwey-Overbeek) interactions probably playing an important role. AFM tips comprising well-defined silica colloidal particles have been used to measure the adhesion of lactose carriers [78], and to obtain maps of adhesion between an individual lactose particle and gelatin capsules [79].

4. Final Remarks

Atomic force spectroscopy (AFS) has become one of the most important techniques of the family of surface probe microscopes (SPMs), for it allows the investigation of surface forces at the nanometer scale. Strong binding of some biologically-relevant molecules, for instance, can now be probed at the molecular level. The possibility of generating adhesion maps has also brought unprecedented information about heterogeneities on sample surfaces with nanometer resolution. This also permits investigations on surface contamination, especially in cases of submonolayer coverage.

In this chapter we mentioned a number of applications for AFS in several fields. Perhaps its largest impact will be in nanotechnology, since in the nanoscale the relative importance of the different forces is changed completely. While in the macroscopic world van der Waals forces are not strongly manifested, they are the prime component for intra- and intermolecular interactions. Moreover, AFS is today the most important technique to study van der Waals interactions and adhesion forces. The brief results presented in this chapter demonstrate the range and the complexity of the subject and they bring out the importance for investigations in the field of nanoscience and nanotechnology, due to the challenges as well as the wealth of information that, which can be derived from the experiments, as well as from theoretical models.

Acknowledgements. The financial support by CNPq, FINEP, FAPESP, Embrapa Agricultural Instrumentation, Embrapa-Labex (Brazil) and IFSC/USP (São Carlos) is gratefully acknowledged.

References

- [1] C.-J. Zhong, L. Han, M. M. Maye, J. Lou, N. N. Kariuki and W. E. Jones, Jr. *J. Chem. Educ.* **80**, 194 (2003).
- [2] J. C. Wright, *J. Chem. Educ.* **73** 827 (1996).
- [3] K. Aumann, K. J. C. Muyskens, K. Sinniah, *J. Chem. Educ.* **80** 187 (2003).
- [4] G. Binnig, H. Rohrer, Ch. Gerber and E. Weibel, *Appl. Phys. Lett.* **40**, 178 (1982).
- [5] G. Binnig, C. F. Quate and C. Gerber, *Phys. Rev. Lett.* **56**, 930 (1986).
- [6] V. J. Morris, *Prog. Biophys. Molec. Biol.* **61** 131 (1994).
- [7] F. L. Leite, L. G. Paterno, C. E. Borato, P. S. P. Herrmann, O. N. Oliveira and L. H. C. Mattoso, *Polymer* **46** 12503 (2005).
- [8] M. A. Mosiewicki, W. F. Schroeder, F. L. Leite, P. S. P. Herrmann, A. A. S. Curvelo, M. I. Aranguren, J. Borrajo. *J. Mat. Sci.* **41** 6154 (2006).
- [9] F. L. Leite, A. Riul Jr and P. S. P. Herrmann, *J Adhesion Sci. Technol.* **17**, 2141 (2003).
- [10] L. Sirghi, N. Nakagiri, K. Sugisaki, H. Sugimura, and O. Takai, *Langmuir* **16**, 7796 (2000).
- [11] W. Szuskiewicz, B. Hennion, M. Jouanne, J. F. Morhange, E. Dynowska, E. Janik and T. Wojtowicz, *J. Magn. and Magn.. Mater.* **197**, 425 (1999).
- [12] N. C. Santos and M. A. R. B. Castanho, *Biophys. Chem.* **107**, 133 (2004).
- [13] A. Ikai, *Surf. Sci. Rep.* **26**, 261 (1996).
- [14] C. E. Borato, F. L. Leite, O. N. Oliveira Jr, R. C. Goy, S. P. Campanha Filho, C. L. Vasconcelos, C. G. da Trindade Neto, M. R. Pereira, J. L. C. Fonseca, L. H. C. Mattoso, *IEEE Trans. Dielec. Elec. Insulation* **13** 1101 (2006).
- [15] N. C Souza, J. R. Silva, M. A. Pereira-da-Silva, M. Raposo, R. M. Faria., J. A. Giacometti and O. N. Oliveira Jr, *J. Nanosci. Nanotechnol.* **4**, 1 (2004).
- [16] M. Noeske, J. Degenhardt, S. Strudthoff and U. Lommatzsch, *Int. J. Adhesion Adhes.* **24**, 171 (2004).
- [17] E. Evans, *Annu. Rev. Biophys. Biomolec. Struct.* **30**, 105 (2001).
- [18] Y. F. Dufr nem, C. J. P. Boonaert, H. C. van der Mei, H. J. Busscher and P. G. Rouxhet, *Ultramicroscopy* **86**, 113 (2001).
- [19] J. K. Gimzewski, *Science* **283**, 1683 (1999).
- [20] V. N. Blisnyuk, H. E. Assender and G. A. D. Briggs, *Macromolecules* **35**, 6613 (2002).
- [21] K. Nakajima, H. Yamaguchi, J.-C. Lee, M. Kageshima, T. Ikehara and T. Nishi, *Jpn. J. Appl. Phys.* **36**, 3850 (1997).
- [22] P. Attard, *J. Adhesion Sci. Technol.* **16**, 753 (2002).
- [23] F. Mugele, T. Becker, R. Nikopoulos, M. Kohonen and S. Herminghaus, *J. Adhesion Sci. Technol.* **16**, 951 (2002).
- [24] F. L. Leite and P. S. P. Herrmann, *Acta Microscopica* **12** (A)130 (2003).
- [25] G. Meyer, and N. M. Amer, *Appl. Phys. Lett.* **53**, 1045 (1988).
- [26] S. Alexander, L. Hellemsans, O. Marti, J. Schneir, V. Elings, P. K. Hansma, M. Lonhmire and J. Gurley, *J. Appl. Phys.* **65**, 164 (1989).
- [27] F. L. Leite, P. S. P. Herrmann, *J. Adhesion Sci. Technol.* **19** 365 (2005).
- [28] S. N. Magonov and D. H. Reneker, *Annu. Rev. Mater. Sci.* **27**, 175 (1997).
- [29] P. A. Maurice, *Colloid Surf. A* **107**, 57 (1996).
- [30] K. Cooper, A. Gupta, and S. Beaudoin, *J. Colloid Interf. Sci.* **228**, 213 (2000).
- [31] N. A. Burnham, R. J. Colton and H. M. Pollock, *Nanotechnology* **4**, 64 (1993).
- [32] B. Cappella, and G. Dietler, *Surf. Sci.* **34**, 1 (1999).
- [33] M. B. Viani, T. S. Sch ffer, A. Chand, M. Rief, H. E. Gaub and P. K. Hansma, *J. Appl. Phys.* **86**, 2258 (1999).
- [34] J. H. Hoh, J. P. Cleveland, C. B. Prater, J. P. Revel and P. K. Hansma, *J. Am. Chem. Soc.* **114**, 4917 (1992).
- [35] W. F. Heinz and J. H. Hoh, *Trends Biotechnol.* **17**, 143 (1999).
- [36] G. U. Lee, D. A. Kidwell and R. J. Colton, *Langmuir* **10**, 354 (1994).
- [37] N. A. Burnham, D. D. Dominguez, R. L. Mowery and R. J. Colton, *Phys. Rev. Lett.* **64**, 1931 (1990).
- [38] A. Tonck, J. L. Loubet, and J. M. Georges, *ASLE Trans.* **29**, 532 (1986).
- [39] N. A. Burnham and R. J. Colton, *J. Vac. Sci. Technol. A* **7**, 2906 (1989).
- [40] C. B. Prater, P. G. Maivald, K. J. Kjoller, M. G. Heaton, in: *probing nano-scale forces with the atomic force microscope*, © Veeco Instruments Inc. All rights reserved. Santa Barbara, California, 1995, pp. 16.
- [41] E. Meyer, *Prog. Surf. Sci.* **41**, 3 (1992).
- [42] J. P. Cleveland, S. Manne, D. Bocek and P. K. Hansma, *Rev. Sci. Instrum.* **64**, 403 (1993).
- [43] J. E. Sader, I. Larson, P. Mulvaney and L. R. White, *Rev. Sci. Instrum.* **66**, 3789 (1995).
- [44] J. L. Hutter and J. Bechhiefer, *Rev. Sci. Instrum.* **64**, 1868 (1993).

- [45] R. Lévy and M. Maaloum, *Nanotechnology* **13**, 33 (2002).
- [46] F. L. Leite, C. E. Borato, W. T. L. da Silva, P. S. P. Herrmann, O. N. Oliveira and L. H. C. Mattoso, *in press*, *Microsc. Microanal.* **13** (4) (2007).
- [47] C. E. Borato, F. L. Leite, O. N. Oliveira and L. H. C. Mattoso, *Sensor Lett.* **4**, 155 (2006).
- [48] C. Rotsch and M. Radmacher, *Langmuir* **13**, 2825 (1997).
- [49] M. Radmacher, J. P. Cleveland, M. Fritz, H. G. Hansma and P. K. Hansma, *Biophys. J.* **66**, 2159 (1994).
- [50] H. A. Mizes, K. G. Loh, R. J. D. Miller, S. K. Ahuja and E. Grabowski, *Appl. Phys. Lett.* **59**, 2901 (1991).
- [51] G. A. Willing, T. H. Ibrahim, F. M. Etzler and R. D. Neuman, *J. Colloid Interf. Sci.* **226**, 185 (2000).
- [52] P. Taboada-Serrano, V. Vithayaveroj, S. Yiacoumi, C. Tsouris, *Environ. Sci. Technol.* **39**, 6352 (2005).
- [53] O. H. Willemsen, M. M. E. Snel, L. Kuipers, C. G. Figdor, J. Greve, B. G. De Grooth, *Biphys. J.* **76**, 716 (1999).
- [54] F. L. Leite, E. C. Ziemath, O. N. Oliveira and P. S. P. Herrmann, *Microsc. Microanal.* **11**, 130 (2005).
- [55] N. Consolin Filho, F. L. Leite, E. R. Carvalho, E. C. Venancio, C. M. P. Vaz, L. H. C. Mattoso, *in press*, *J. Braz. Chem. Soc.* **18**, 577 (2007).
- [56] F. L. Leite, P. S. P. Herrmann, A. L. Da Róz, F. C. Ferreira, A. A. S. Curvelo and L. H. C. Mattoso, *J. Nanosci. Nanotechnol.* **6**, 2354 (2006).
- [57] T. Nakagawa, K. Ogawa, S. Kurumizawa and T. Ozaki, *Jpn. J. Appl. Phys.* **32**, L294 (1993).
- [58] C. D. Frisbie, L. F. Rozsnai, A. Noy, M. S. Wrighton and C. M. Lieber, *Science* **265**, 2071 (1994).
- [59] R. Mckendry, M.-E. Theoclitou, C. Abell and T. Rayment, *Jpn. J. Appl. Phys.* **38**, 3901 (1999).
- [60] D. A. Smith, S. D. Connel, C. Robinson and J. Kirkham, *Anal. Chim. Acta* **479**, 39 (2003).
- [61] E.-L. Florin, V. T. Moy and H. E. Gaub, *Science* **264**, 415 (1994).
- [62] G. W. Tormoen, J. Drelich and E. R. Beach, *J. Adhesion Sci. Technol.* **18**, 1 (2004).
- [63] R. Raiteri, M. Grattarola, and R. Berger, *Mater. Today* **5**, 22 (2002).
- [64] D. V. Vezenov, A. Noy, L. F. Roznyai and C. M. Lieber, *J. Am. Chem. Soc.* **119**, 2006 (1997).
- [65] R. S. Abendan and J. A. Swift, *Langmuir* **18**, 4847 (2002).
- [66] N. J. Brewer, B. D. Beake and G. J. Leggett, *Langmuir* **17**, 1970 (2001).
- [67] C. Ton-That, P. A. Campbell and R. H. Bradley, *Langmuir* **16**, 5054 (2000).
- [68] M. C. Roggemann and J. G. Williams, *J. Adhesion Sci. Technol.* **16**, 905 (2002).
- [69] M. Florini, R. McKendry, M. A. Cooper, T. Rayment and C. Abell, *Biophys. J.* **80**, 2471 (2001).
- [70] M. E. Browning-Kelley, K. Wadu-Mesthrige, V. Hari and G. Y. Liu, *Langmuir* **13**, 343 (1997).
- [71] V. Mangipudi, M. Tirrell and A. V. Pocius, *J. Adhesion Sci. Technol.* **8**, 1251 (1994).
- [72] M. Giesbers, J. M. Kleijn and M. A. C. Stuart, *J. Colloid and Interf. Sci.* **248**, 88 (2002).
- [73] W. R. Bowen, N. Hilal, R. W. Lovitt and C. J. Wright, *Colloid and Surface A* **157**, 117 (1999).
- [74] T. H. Ibrahim, T. R. Burk, F. M. Etzler and R. D. Neuman, *J. Adhesion Sci. Technol.* **14**, 1225 (2000).
- [75] W. A. Ducker, T. J. Senden and R. M. Pashely, *Nature* **353**, 239 (1991).
- [76] H.-J. Butt, *J. Colloid Interface Sci.* **166**, 109 (1994).
- [77] M. Kappl, H.-J. Butt, *Part. Part. Syst. Charact.* **19**, 129 (2002).
- [78] M. D. Louey, P. Mulvaney and P. J. Stewart, *J. Pharm. Biomed. Anal.* **25**, 559 (2001).
- [79] G. A. Willing, T. A. Ibrahim, F. M. Etzler and R. D. Neuman, *J. Colloid Interf. Sci.* **226**, 185 (2000).